Linear Collider Collaboration Tech Notes

Resolution and Systematics in Beam-based Alignment of a Long, Periodic Beam Line

February 4, 1999

P. Tenenbaum
Stanford Linear Accelerator Center
Stanford, CA

Abstract:

The beam-based alignment algorithm for the NLC main linac requires that the magnetic-electrical offset between the center of each BPM and the center of its quadrupole be determined with an absolute accuracy on the order of microns via quadrupole shunting; this allows the quads to be moved such that the beam is passing through the quad centers to this accuracy. In this note we consider the range over which each quadrupole must be shunted to achieve a 1 μs statistical resolution, given certain features of the lattice and assumptions about the shunting pattern and amount of data to be acquired. We give an expression for the amount that the quadrupole's center can shift during shunting if the systematic error on the determination of the center of the quad at its operating strength is to be held to 1 \u. Finally we present a model of the expected quad center shifting due to unequal permeability of the 4 pole-pieces, and conclude that with some caution in the shunting technique the tolerance on this effect can be achieved.

Resolution and Systematics in Beam-Based Alignment of a Long Periodic Beamline

Peter Tenenbaum
LCC-Note-0006
Draft 19-October-1998

Abstract

The beam-based alignment algorithm for the NLC main linac requires that the magnetic-electrical offset between the center of each BPM and the center of its quadrupole be determined with an absolute accuracy on the order of microns via quadrupole shunting; this allows the quads to be moved such that the beam is passing through the quad centers to this accuracy. In this note we consider the range over which each quadrupole must be shunted to achieve a 1 μ statistical resolution, given certain features of the lattice and assumptions about the shunting pattern and amount of data to be acquired. We give an expression for the amount that the quadrupole's center can shift during shunting if the systematic error on the determination of the center of the quad at its operating strength is to be held to 1 μ. Finally we present a model of the expected quad center shifting due to unequal permeability of the 4 pole-pieces, and conclude that with some caution in the shunting technique the tolerance on this effect can be achieved.

1 Introduction

Alignment of the quadrupoles and the RF structures in the NLC main linac to the beam is a prerequisite for delivering the desired emittances to the beam delivery system. The canonical algorithm for performing this alignment has been elicudated elsewhere [1], and we summarize it here:

- Each quad in the linac is shunted, and the resulting deflection on downstream BPMs is recorded; from the deflection as a function of quad strength the quad misalignment is computed; the BPM offset is computed by adding the BPM reading to the quad misalignment
- The BPM offsets are added to the database and the quads are moved to positions which zero the BPM readings
- The RF structures are aligned by moving the girders until the average reading of 6 BPMs (one at the upstream end and one at the downstream end of each structure) is zero (it is assumed that the structure BPMs will have zero offset because they look directly at the power in the HOM couplers rather than comparing two signals as the quad BPMs do)
- The steps above are iterated as necessary.

In order to converge, the algorithm requires that the BPM offsets can be determined to an absolute accuracy on the order of microns; the NLC steering simulations typically assume that the RMS BPM offset is 2 microns [2]. Since the accuracy of the BPM offset is equal to the accuracy with which the quadrupole misalignment is determined, several issues related to the quadrupole-shunting technique present themselves:

- Over how large a range must each quad in the NLC main linac be shunted in order to achieve a given statistical resolution of the misalignment?
- In the event that the magnetic center of the quad changes during shunting, what is the limit on this effect to achieve a given systematic error?
- Can the limits on the quad center shift during shunting be reasonably achieved by iron-dominated quads?

In this note we attempt to answer the questions above.

2 Statistical Resolution Limit

Assume a system as diagrammed in Figure 1: the beam passes through a quad with an offset x_0. The deflection at a downstream BPM is:

$$x(i) = x_0 K_q R_{12}(i), \tag{1}$$

where K_q is the quadrupole integrated strength (in m^{-1}), and $R_{12}(i)$ is the R_{12} matrix element from the quad to the ith BPM. If the quad strength is varied in several steps, where each step changes the strength by dK_q, then the change in the downstream deflection is given by:

$$dx(i,j) = x_0 j dK_q R_{12}(i), \tag{2}$$

where j is the step index.

If we now form a least-squares model involving many BPMs and many values of j, we find the following expression for χ^2:

$$\chi^2 = \frac{1}{\sigma^2_{\mathrm{BPM}}} \sum_i \sum_j \left[dx(i,j) - x_0 j dK_q R_{12}(i) \right]^2 . \tag{3}$$

Minor manipulation of derivatives reveals that the value of x_0 can be fitted with an expected resolution given by:

$$\sigma_x^2 = \frac{\sigma^2_{\mathrm{BPM}}}{\sum_i \sum_j j^2 dK_q^2 R_{12}^2(i)}. \tag{4}$$

We can simplify Equation 4 by noting that the only term dependent on i in the equation is $R_{12}^2(i)$. In a periodic FODO lattice, we can replace $\sum_i R_{12}^2(i)$ with $n\mathcal{R}$, where $\mathcal{R}$ is the sum of $R_{12}^2(i)$ over half a betatron wavelength and n is the number of half-wavelengths used in the fit. Thus Equation 4 becomes:

$$\sigma_x^2 = \frac{\sigma^2_{\mathrm{BPM}}}{n\mathcal{R} dK_q^2 \sum_j j^2}. \tag{5}$$

It is important to remember that Equation 5 is for a single pulse on each step of the quad, and that the resolution improves with the familiar $1/\sqrt{N_{\mathrm{pulse}}}$ as averaging over many pulses is used.

Let us apply Equation 5 to the most recent NLC lattice. The lattice consists of 3 "supersectors," in which the separation between quadrupoles increases from 1 RF girder to 3 RF girders and each girder contains 3 of the 1.8 meter structures. The phase advance per cell is tapered, with a larger phase advance per cell at the start of each supersector than at the end, and a larger phase advance in the vertical than in the horizontal. Consequently the resolution at the downstream end of each supersector will be somewhat different than the resolution at the upstream end, and the horizontal and vertical planes will have slightly different resolutions.

Let us consider shunting an F quad at the beginning and end of each supersector. The BPM resolution is assumed to be 1μ, and the scan will consist of 5 steps, arranged either symmetrically (in which case $j \in \{-2,-1,0,1,2\}$) or asymmetrically (in which case $j \in \{0,1,2,3,4\}$). The target statistical resolution is 1μ. Table 1 shows the necessary scan ranges needed to achieve the resolution in x and y with no averaging and using only 1 betatron half-wavelength.

Table 1: Quad Strength Excursions for Beam-Based Alignment Resolution

Region	K_q m^{-1}	$\sum R_{12}^2$ m^2	$\sum R_{34}^2$ m^2	Symmetric dK_q, m^{-1} (x)	Symmetric dK_q, m^{-1} (y)	Asymmetric dK_q, m^{-1} (x)	Asymmetric dK_q, m^{-1} (y)
1 Start	0.0243	560	87	0.0134	0.0334	0.0077	0.0196
1 End	0.0175	867	216	0.0107	0.0215	0.0062	0.0124
2 Start	0.0125	2219	199	0.0067	0.0224	0.0039	0.0129
2 End	0.0095	3092	683	0.0057	0.0121	0.0033	0.0070
3 Start	0.0078	4138	789	0.0049	0.0113	0.0028	0.0065
3 End	0.0078	5392	761	0.0043	0.0115	0.0025	0.0066

As one might expect, the range needed to align an F quad in the vertical is much larger than that needed in the horizontal. The ranges for aligning a D quad in the vertical and horizontal are nearly the same as those needed for an F quad in horizontal and vertical, respectively, and are not shown.

For a single BPM reading per step and a single betatron half-wavelength, the step size needed is frequently larger than the design strength of the quadrupole, which is neither optimal nor realistic. A somewhat more realistic model is one in which several betatron wavelengths are used and BPM averaging is also allowed. The choice of the number of betatron wavelengths should be as large as possible, but not so large that model errors or wakefield kicks begin to dominate the deflection measurements. We somewhat arbitrarily choose 5 betatron half-wavelengths. Similarly the number of averaged pulses should be as large as possible but small enough to be acquired quickly relative to the rate at which the accelerator is changing due to mechanical or electrical drifts. We have chosen 144 pulses per quad step, which can be acquired in 1.2 seconds at full machine rate. Table 2 shows the total range of quad shunt needed as a percentage of the standard operating strength in order to achieve the desired resolution with the averaging outlined above. Note that the range shown for a symmetric scan is from the operating point to the maximum excursion in one direction, *i.e.*, a symmetric x range of 4.1% means that the BPMs are sampled for the quad at -4.1%, -2.05%, 0%, 2.05%, and 4.1% deviation from the standard strength. Thus the *total* shunt ranges for symmetric scans are larger than for asymmetric ones, but the maximum deviation from the operating point is usually somewhat smaller.

Table 2: Maximum quad strength excursions to achieve 1μ precision, NLC Beam-Based Alignment.

Region	Symmetric x range	Symmetric y range	Asymmetric x range	Asymmetric y range
1 Start	4.1%	10.2%	4.7%	12.0%
1 End	4.6%	9.2%	5.3%	10.6%
2 Start	4.0%	12.8%	4.7%	15.4%
2 End	4.5%	9.5%	5.2%	11.0%
3 Start	4.7%	10.8%	5.4%	12.4%
3 End	4.1%	11.0%	4.8%	12.6%

3 Quadrupole Offset Shifts

One likely source of systematic error in the quad-shunting alignment procedure is that the magnetic center of the quadrupole may change as a function of excitation current. This may happen because of thermal changes as the current increases or decreases, changing magnetic forces within the magnet causing a distortion, or varying permeabilities of the 4 pole-pieces causing the center to "wander."

Consider a quad whose magnetic center at its design strength is at x_0, and which is given at step j of the quad scan by $x_0 + x_j$; for $j = 0$, $x_j \equiv 0$. The deflection on a downstream BPM on step j is given in this case by:

$$x(i,j) = (x_0 + x_j)(K_q + jdK_q)R_{12}(i), \tag{6}$$

which means that the change in deflection at the downstream BPM from the deflection when the quad is at its operating point is:

$$dx(i,j) = \left[(x_0 + x_j)jdK_q + x_jK_q\right] R_{12}(i). \tag{7}$$

The model to which the data is fitted does not allow for the center shifting:

$$dx(i,j)_M = (x_M)jdK_qR_{12}(i). \tag{8}$$

If we again construct a χ^2 and find the value of x_M which minimizes it, then the relationship between the fitted quadrupole offset and the actual quad offset at the operating point is given by:

$$x_M - x_0 = \frac{\sum_j j^2 x_j}{\sum_j j^2} + \frac{K_q \sum_j j x_j}{dK_q \sum_j j^2}. \tag{9}$$

Does Equation 9 make sense? Consider first the case in which two strengths are used to determine the quad's offset: its operating point and zero strength. In this case $dK_q = K_q$, $j = -1$, and Equation 9 indicates that no error occurs in the fitted magnet offset due to the center shifting; this is commonsensical, since if the magnet is actually off the motions of its magnetic center cannot perturb the beam.

Another limiting case is the one in which a very small change in the quad strength moves the center a large distance. In this case the change in the quad center is magnified by K_q/dK_q; as we expect, if the magnet center moves substantially when the quad is shunted by a tiny fraction of its strength, the fit error will be enormous.

4 Center Shifts due to Permeability Mismatch

One possible cause of shifts in the magnetic center of a quad as a function of quad strength is that the B versus I curves of the four pole-pieces are different from one another, which arises from mismatches in the permeability of the pole-pieces. We can achieve some insight into this phenomenon by resorting to the magnetic multipole expansion.

Consider the system in Figure 2: a mechanically perfect quadrupole is constructed, and each pole is then excited to a different strength. The magnetic scalar potential, Φ, within the magnet aperture is given by a series expansion in the relevant harmonics [3]:

$$\Phi = \sum_n A_n r^n \sin n\theta + \sum_n B_n r^n \cos n\theta. \tag{10}$$

Assuming that each pole-piece is mechanically perfect and that the permeability is high enough to be effectively infinite, each pole-piece is an equipotential. This is a boundary condition for Equation 10 which can be expressed thus:

$$\begin{aligned}
\Phi = \Phi_1,\ r^2 \sin 2\theta = a^2,\ \theta \in \left[0, \frac{\pi}{2}\right), \\
\Phi = \Phi_2,\ r^2 \sin 2\theta = -a^2,\ \theta \in \left[\frac{\pi}{2}, \pi\right), \\
\Phi = \Phi_3,\ r^2 \sin 2\theta = a^2,\ \theta \in \left[\pi, \frac{3\pi}{2}\right), \\
\Phi = \Phi_4,\ r^2 \sin 2\theta = -a^2,\ \theta \in \left[\frac{3\pi}{2}, 2\pi\right).
\end{aligned} \tag{11}$$

We can use Equation 10 to express the magnetic potential at the boundary by replacing r with $a/\sqrt{|\sin 2\theta|}$:

$$\Phi_{\text{boundary}} = \sum_n A_n \frac{a^n \sin n\theta}{|\sin 2\theta|^{n/2}} + \sum_n B_n \frac{a^n \cos n\theta}{|\sin 2\theta|^{n/2}}. \tag{12}$$

We can project out the A_n components by multiplying Φ by $\sin m\theta |\sin 2\theta|^{n/2}$ and integrating from zero to 2π. By the orthogonality relation for $\sin n\theta$ this will yield $A_n a^n \pi \delta_{mn}$. Since Equation 11 expresses the value of the potential along the boundary, we can multiply this expression of the potential by $\sin m\theta |\sin 2\theta|^{n/2}$, integrate around a full circle, and set the result equal to $A_n a^n \pi \delta_{mn}$ in order to obtain A_n:

$$\begin{aligned}
\int_0^{\pi/2} \Phi_1 \sin n\theta |\sin 2\theta|^{n/2} \quad + \quad \int_{\pi/2}^{\pi} \Phi_2 \sin n\theta |\sin 2\theta|^{n/2} + \\
\int_{\pi}^{3\pi/2} \Phi_3 \sin n\theta |\sin 2\theta|^{n/2} \quad + \quad \int_{3\pi/2}^{2\pi} \Phi_4 \sin n\theta |\sin 2\theta|^{n/2} = A_n a^n \pi.
\end{aligned} \tag{13}$$

Evaluating Equation 13 yields:

$$\begin{aligned}
A_1 &= \frac{1}{4}\left(\Phi_1 + \Phi_2 - \Phi_3 - \Phi_4\right), \\
B_1 &= \frac{1}{4}\left(\Phi_1 - \Phi_2 - \Phi_3 + \Phi_4\right),
\end{aligned} \tag{14}$$

$$\begin{aligned} A_2 &= \frac{1}{4}\left(\Phi_1 - \Phi_2 + \Phi_3 - \Phi_4\right), \\ B_2 &= 0, ... \end{aligned}$$

Naturally if the 4 poles are each excited to different strengths there will be higher harmonics than the quadrupole terms; however, the higher harmonics do not generate magnetic fields at the mechanical center of the magnet – only the dipole harmonics can do this. If the differential excitation of the poles is small relative to the quadrupole excitation, then we can neglect the effects of higher-order terms in moving the "neutral axis" of the magnet (the point in (x, y) space where $B_x = B_y = 0$) and approximately locate the magnetic center at the point where the sum of the dipole and quadrupole fields is nulled.

Let us further decompose the individual excitations of the 4 poles as shown in Figure 3: here the excitation of each pole piece is the sum of a magnetic potential for the quadrupole field, the magnetic potential for a horizontal dipole field, and the magnetic potential for a vertical dipole field. We can then rewrite the coefficients in the multipole expansion:

$$\begin{aligned} A_1 &= \Phi_x, \\ B_1 &= \Phi_y, \\ A_2 &= \Phi_q, \\ B_2 &= 0. \end{aligned} \tag{15}$$

To lowest order, the magnetic scalar potential in cartesian coordinates becomes:

$$\Phi = \frac{\Phi_y}{a}x + \frac{\Phi_x}{a}y + \frac{\Phi_q}{a^2}2xy. \tag{16}$$

When we compute the magnetic fields by taking $\vec{\nabla}\Phi$ and requiring that $|\vec{B}| = 0$, we find that the magnetic center's position is given by:

$$\frac{x}{a} = \frac{-\Phi_x}{2\Phi_q}, \ \frac{y}{a} = \frac{-\Phi_y}{2\Phi_q}. \tag{17}$$

5 Simulation of Permeability Mismatches

In order to study the effects of permeability mismatches on beam-based alignment, we have used the B versus I behavior of the FFTB standard quadrupoles as a model for the different Φ values of the pole-pieces. The FFTB standard quads are solid-core magnets, and their magnetic gradients as a function of current have been characterized up to a current of 240 amperes (corresponding to a pole-tip field of 9.6 kG). Figure 4 shows the B versus I behavior for a typical quad. We have assumed that the differences in B versus I behavior for the different FFTB quads come from the quads' iron cores having different permeabilities, and that therefore the hysteresis curves of the magnets can serve as a measure of the variability of permeability from one pole-piece to another.

We have fitted the B versus I data for each quad to a polynomial of order 5. In order to simulate a single quadrupole, we select 4 FFTB quads at random, and use their B versus I polynomials to generate Φ versus I data for the 4 pole-pieces of a simulated magnet. On each such simulated magnet we then simulate a quad-shunting scan about setpoints from 25% to 90% of the magnet's full strength, and at each point in the scan evaluate the position of the magnetic center using Equation 17. We then use Equation 9 to evaluate the error in fitting the magnetic center at the operating point due to the center shift from permeability mismatches.

Figure 5 shows the RMS fitting error as a function of quad operating point for small-range quad scans. By "small-range" we mean scans which are adequate for measuring the x offset of an F quad with a statistical resolution of 1μ, as described in Table 2: the scan range for asymmetric scans is 5% of the operating point (so, for example, the scans at 50% of full strength scan from 50% to 52.5% or from 47.5% to 50%), and for symmetric scans the range is $\pm 5\%$ (so from 47.5% to 52.5%). At each operating point 1000 quadrupoles are generated, each with an aperture radius of 5 mm. The values plotted in Figure 5 are twice the "raw" RMS values from the simulation. This is because the FFTB quads contain 4 pole-pieces, and therefore the hysteresis curves of a single quad are assumed to average out some variation in the pole-pieces. Figure 5,

then, is the expected behavior if the 29 FFTB quads were disassembled, and then quads were assembled from 4 pole-pieces selected at random. While the fitting errors for quads operating at relatively weak settings are perhaps tolerable, the errors rise to unacceptable levels for quads that are even at half of their full strength.

Figure 6 shows the RMS fitting error, averaged over 1000 quads per operating point, if the scan range from Figure 5 is doubled. This is roughly the scan range needed to measure the y offset of an F quad to 1μ.

How can the large errors in the quad misalignments be prevented? Equation 9 shows that the problem can be reduced by increasing the scan range and always changing the quad strength to values below its operating point. By doing so, the quad is moved more towards being deactivated, at which strength the fit is completely insensitive to motions of the magnetic center. Figure 7 shows the fit error as a function of shunt range for quadrupoles running at 70%, 80% and 90% of their full strength, again using 5 steps in each scan and 1000 randomly-generated magnets per point on the graph. Figure 7 shows that even very strong quads, if shunted down to 20% of their nominal operating strengths, will have fitting errors of 1μ or less.

6 Conclusions

We have considered several aspects of the beam-based alignment technique anticipated for the Next Linear Collider main linac: the statistical resolution of the procedure, the errors induced by changes in the magnetic center during a quad scan, a mathematical model for quad center shifts due to permeability mismatches, and a simulation study of same. From these we conclude:

- In order to achieve a 1μ statistical resolution on the fitted misalignment of a quad in the main linac, scanning the quad strength over a total range of 5% of the quad's nominal strength is sufficient to measure the x misalignment of an F quad, while 10%-15% is needed to measure the y misalignment of an F quad; this scan range assumes that modest numbers of downstream BPMs and reasonable numbers of pulses are used to fit each quad

- Based on a model for permeability mismatches in the pole-pieces of a quadrupole and data from a set of solid-core quads, the misalignment fit error due to permeability mismatches can be limited to around 0.15% of the quad's aperture radius. In order to achieve this limit, the quads should be shunted from their operating points towards zero strength, and in many cases will need to be reduced to 20% of their normal strengths. Such a large change in the quad strength will drastically change the beam size through the linac, which will potentially alter the beam halo hitting the BPMs and thus introduce another systematic error.

7 Acknowledgements

The authors wish to thank T. Raubenheimer and T. Slaton for many helpful ideas and suggestions.

References

[1] The NLC Design Group, *A Zeroth-Order Design Report for the Next Linear Collider*, (Stanford: SLAC, 1996) 397

[2] R. Assmann *et. al.* "Emittance and Trajectory Control in the Main Linacs of the NLC," SLAC-PUB-7301, in *Proceedings of the 18th International Linac Conference (Linac 96)*, 467-469.

[3] D. C. Carey, *The Optics of Charged Particle Beams*, (New York: Harwood, 1987) 149.

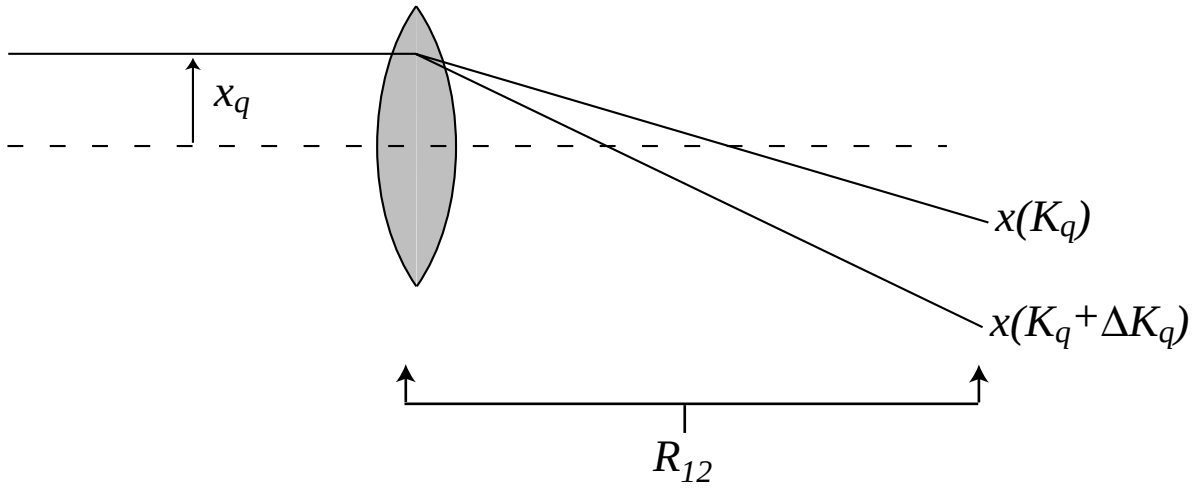

Figure 1: Schematic representation of beam-based quadrupole alignment. The off-axis beam is deflected by the quad; the deflection at a downstream BPM is proportional to the quad strength and the magnet-to-beam offset.

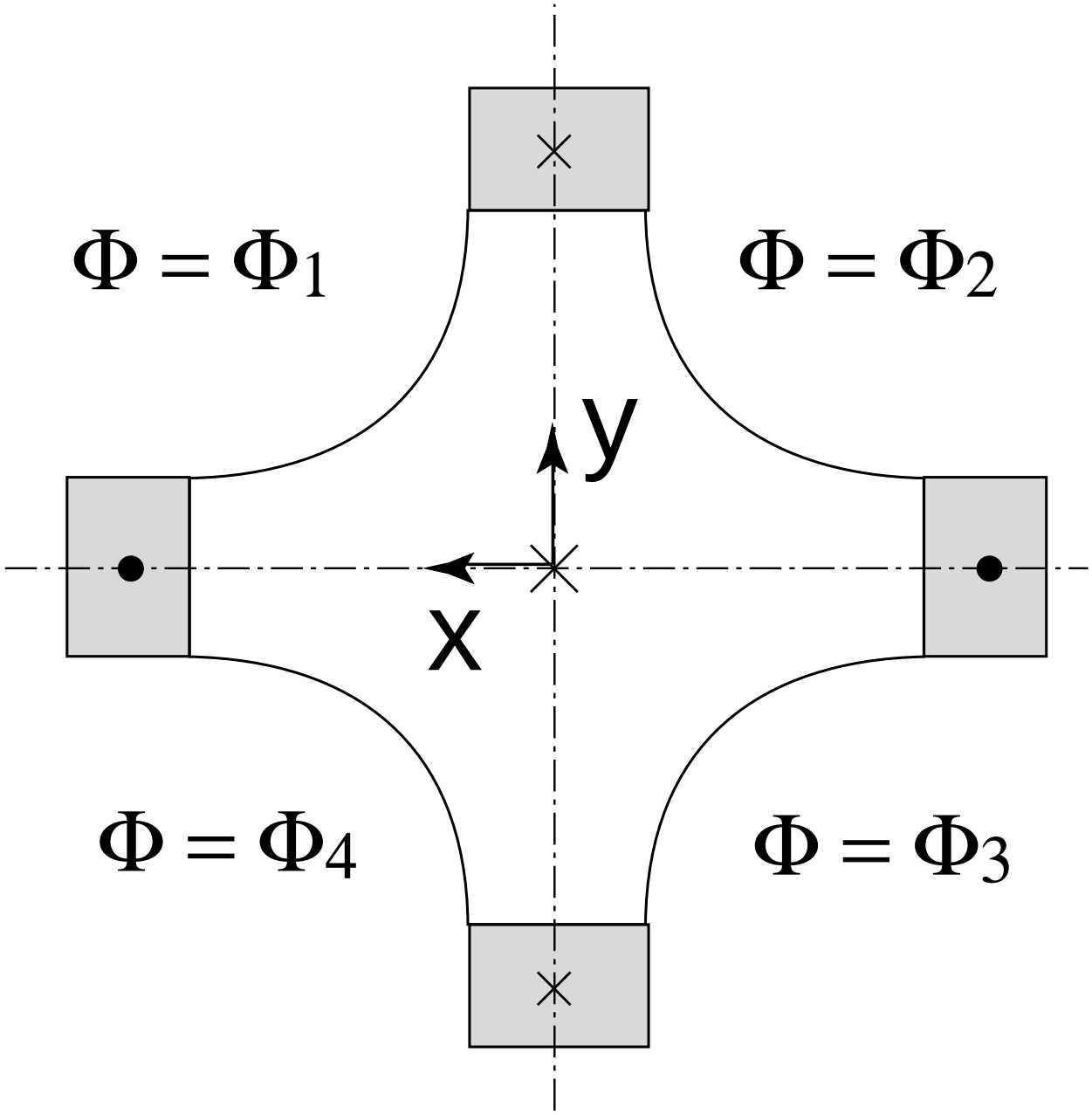

Figure 2: A mechanically perfect quadrupole in which each pole-piece is excited to a different magnetic scalar potential.

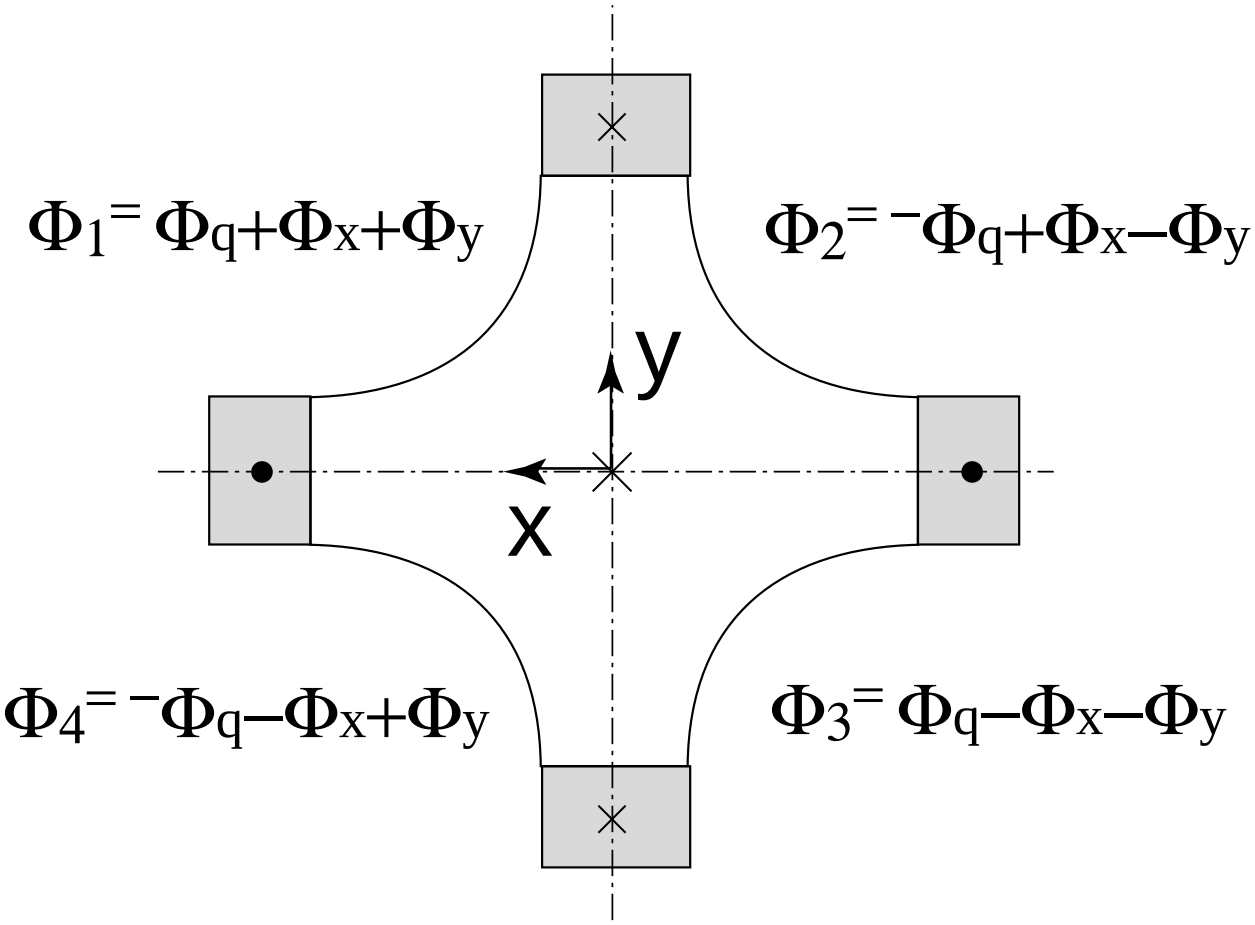

Figure 3: Re-expressing the magnetic scalar potential of each pole as a superposition of dipole and quadrupole potentials.

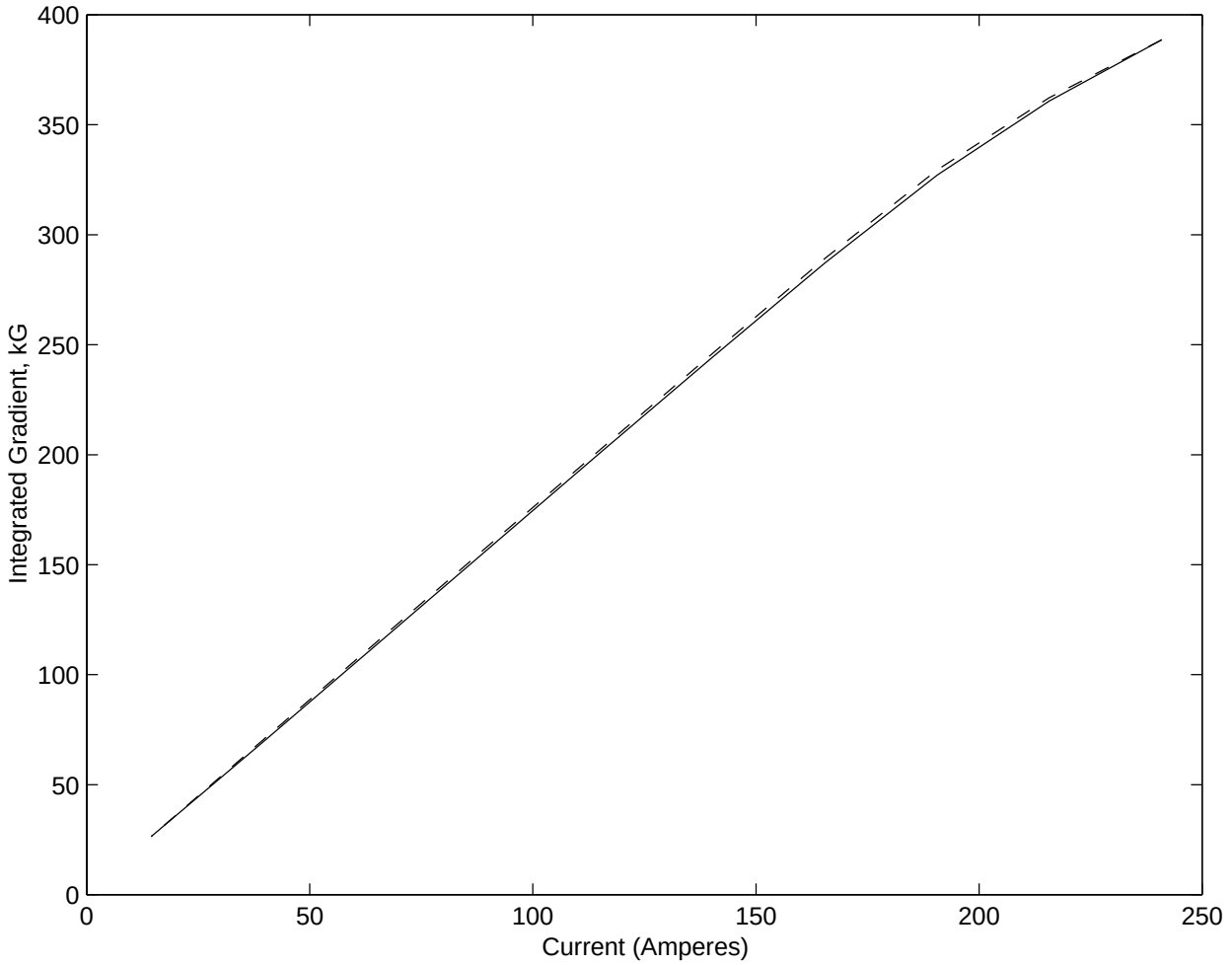

Figure 4: The B versus I curves for a typical FFTB standard quadrupole; both rising (solid) and falling (dashed) curves are shown.

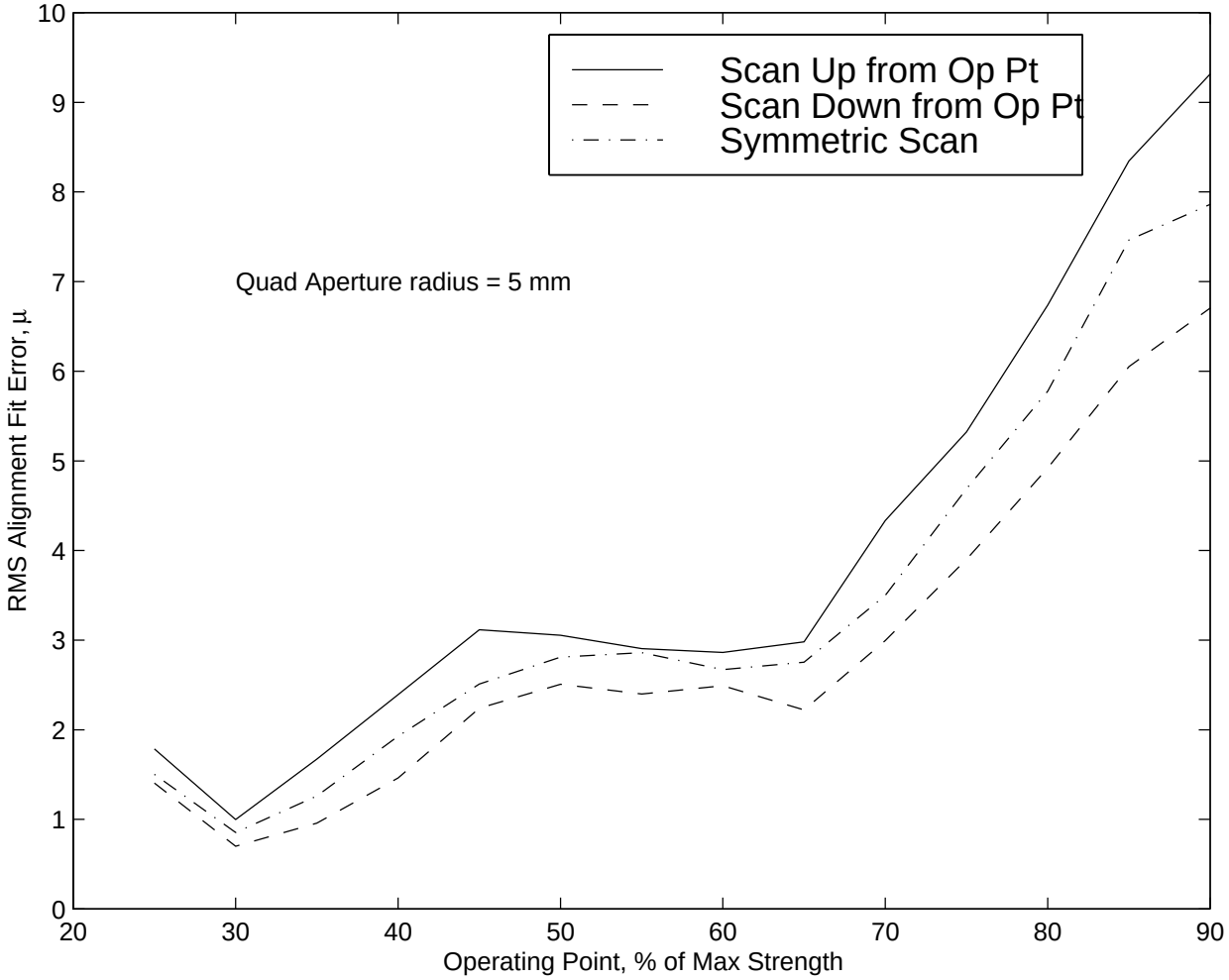

Figure 5: RMS alignment fit errors for simulated quadrupoles assuming small shunting ranges.

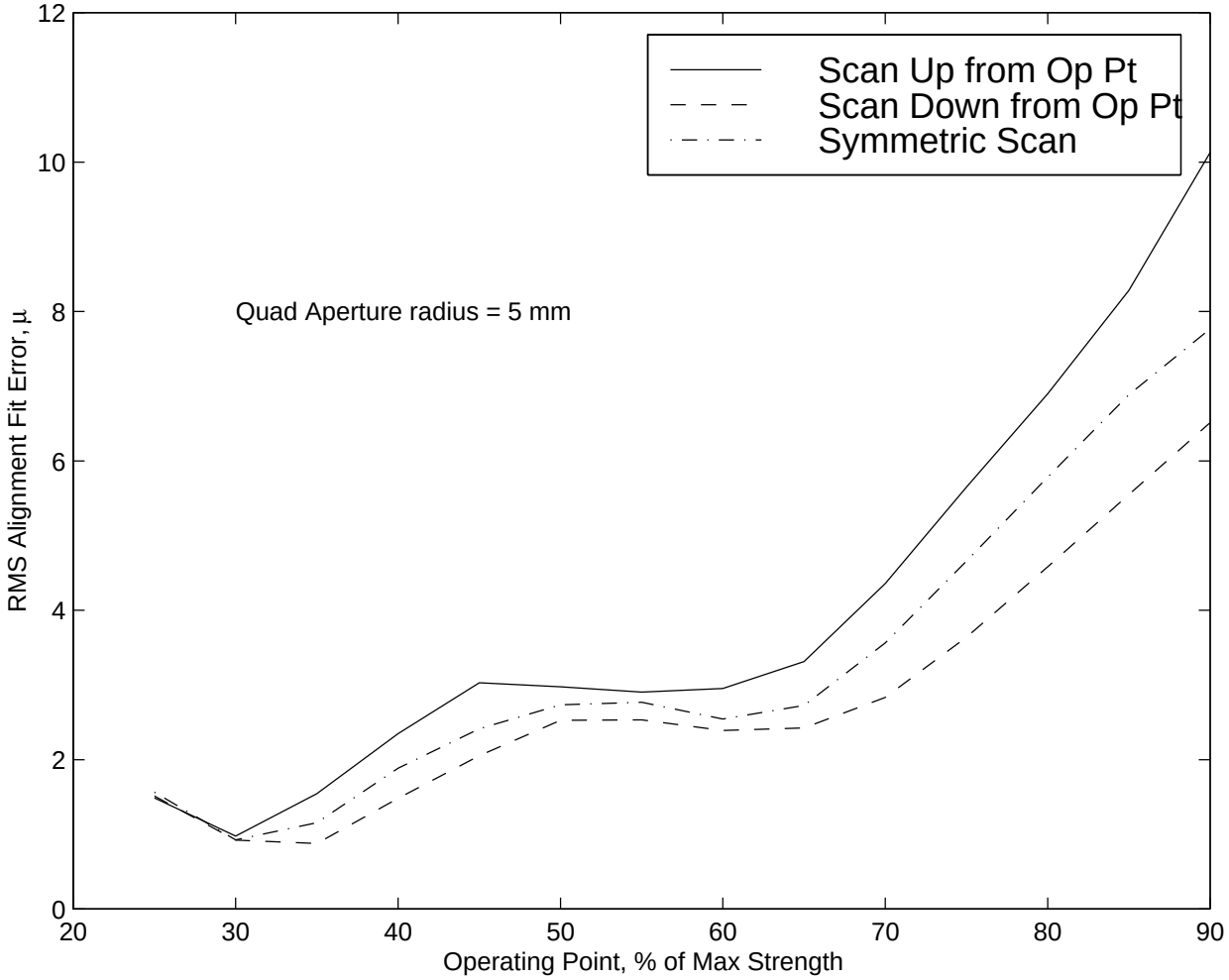

Figure 6: RMS alignment fit errors for simulated quadrupoles assuming large shunting ranges.

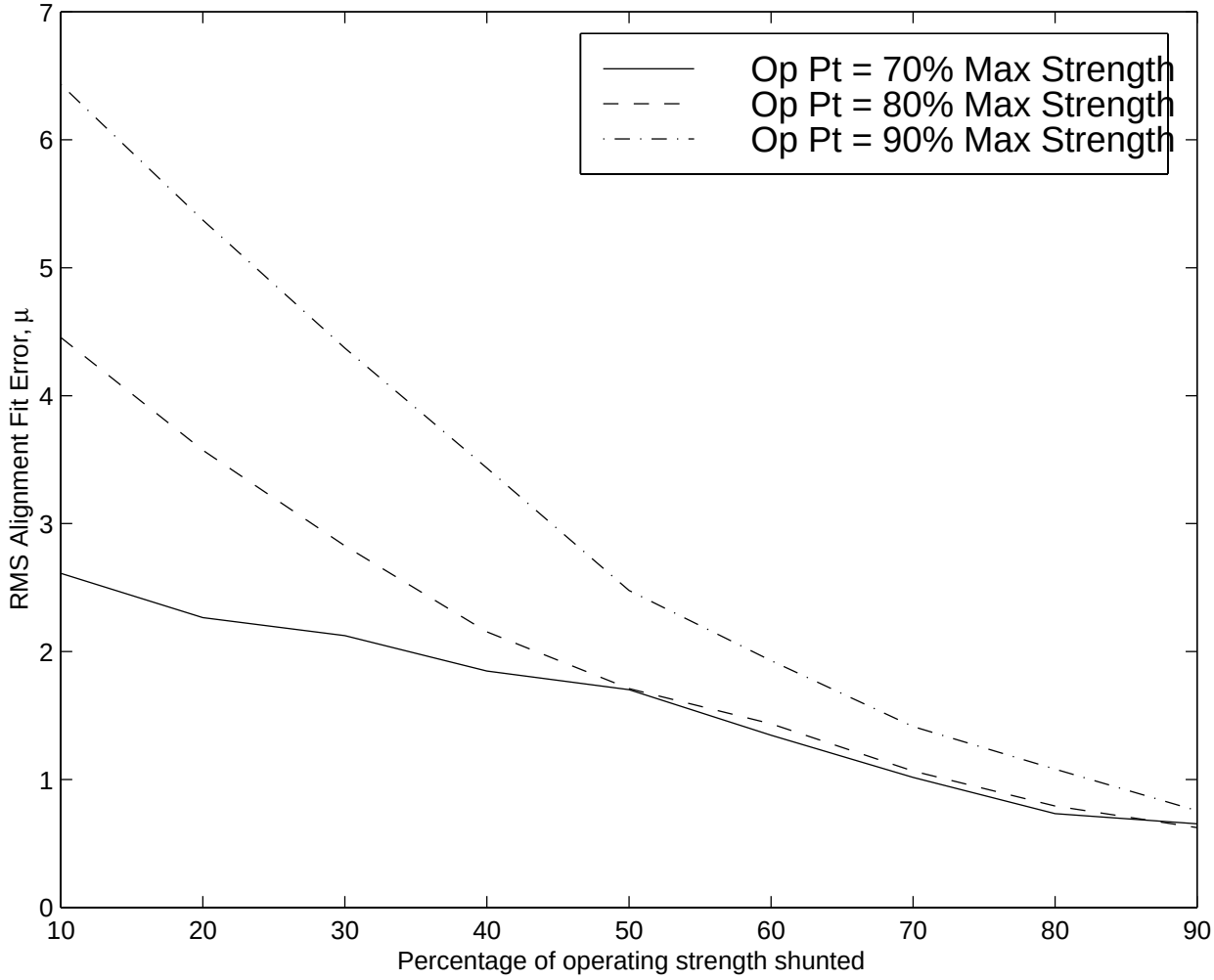

Figure 7: RMS alignment fit errors as a function of total shunt range for several quadrupole nominal strengths.